

(Bipyridine)(terpyridine)(4-iodophenylcyanamide)ruthenium(II) complex: crystallography, electronic absorption spectroscopy, cyclic voltammetry and EPR measurements

Elodie Sondaz, André Gourdon, Jean-Pierre Launay, Jacques Bonvoisin *

Molecular Electronics Group, CEMES/CNRS, 29 Rue Jeanne Marvig, BP4347, 31055 Toulouse Cedex 4, France

Received 4 October 2000; accepted 8 February 2001

Abstract

The complex $[\text{Ru}(\text{bpy})(\text{tpy})(\text{Ipcyd})]^+$ (where bpy: 2,2'-bipyridine, tpy: 2,2':6',2''-terpyridine and Ipcyd: 4-iodophenylcyanamide anion) has been synthesized. An extensive characterization was carried out using IR, ^1H and ^{13}C NMR, ES-MS, UV–Vis, electrochemistry, EPR and X-ray single crystal diffraction analysis. Cyclic voltammogram shows an irreversible anodic peak around 0.7 V/ECS, the shape of the wave is typical of an electrochemical-chemical (EC) mechanism with a half-life time in the order of seconds for the generated species. Oxidation of the title compound has been investigated in order to explore its ability as a magnetic probe for further electronic studies on dinuclear complexes. The EPR spectrum at 100 K of the monooxidized species displays $g_{\perp} = 2.00$ and $g_{\parallel} = 1.96$ attributed to the presence of a radical coming from the phenylcyanamide oxidation, in relative good agreement with EH and ZINDO calculations. © 2001 Elsevier Science B.V. All rights reserved.

Keywords: Ruthenium complexes; Cyanamide complexes; Electrochemistry; Crystal structures

1. Introduction

In the molecular electronics field, it is important to know how the electron, the ultimate source of information at this scale, passes through a molecule, since the goal is to make molecular wires, diodes, switches, etc. The capacity for the electron on going from one side to the other side of the molecule is quantitatively given by the so-called electronic coupling parameter V_{ab} . One can have an experimental access to this parameter by UV–Vis near IR spectroscopy through the intervalence transition in a binuclear complex [1]. This is a rather well established method but it has experimental limits. The most constraining one is associated with the distance between the redox sites in a molecule. Indeed, when this distance is about ca 25 Å, the intervalence transition becomes almost undetectable, i.e. under the sensitivity limit of the apparatus. Therefore, for such long molecules, it is important to find alternative ways

in order to still have access to the degree of the inner electronic communicability. One alternative is to choose paramagnetic compounds and to measure the magnetic coupling between the paramagnetic redox sites through the bridging ligand. There is no doubt that magnetic coupling is another way of measuring the electron communication through a molecule [2]. It remains that the correlation between the magnetic coupling parameter J and the electronic coupling parameter V_{ab} has still to be settled. This magnetic coupling J can be experimentally given by magnetic susceptibility or EPR techniques, this last technique revealing very efficient in some recent examples [3].

The first step in this strategy is to find good candidates giving a strong interaction between distant paramagnetic sites. There are very few systems which satisfy this criterion. R.J. Crutchley found that the NCN group as a coordination site can be the basis for ligands that are extremely efficient to mediate magnetic interaction [4]. Since these ligands are at the same time very efficient for electron transfer within a molecule [5], the NCN group was selected for this study, in association

* Corresponding author. Tel: +33-5-6225 7852; fax: +33-5-6225 7999.

E-mail address: jbonvoisin@cemes.fr (J. Bonvoisin).

with a functionalized part for further extension. Indeed, the iodide group was chosen as an efficient reaction center for further Sonogashira coupling [6]. In this paper, the title diamagnetic Ru(II) complex was firstly synthesized and characterized by crystallography, to develop the synthetic and interpretative tools necessary to obtain long range dinuclear compounds. Secondly its oxidation was studied, with the aim of generating paramagnetic Ru(III) complex.

2. Experimental

2.1. Materials

All chemicals and solvents were reagent grade or better. $[\text{Ru}(\text{tpy})\text{Cl}_3]$ [7] and $[\text{Ru}(\text{tpy})(\text{bpy})\text{Cl}]\text{PF}_6$ [8] were prepared according to literature procedures. 4-Iodoaniline was purchased from Aldrich. RuCl_3 was purchased from Strem Chemicals. Weakly acidic Brockmann I type alumina (Aldrich) was used.

2.2. Measurements

Elemental analyses were performed by the Service d'Analyse du LCC (Toulouse). Electrospray (positive mode) and Electronic Impact mass spectra were obtained with Perkin–Elmer Sciex (Nermag R10-R10). IR were recorded in KBr pellets and nujol mulls on a Perkin Elmer FT-IR 1725. UV–Vis electronic spectra were obtained with a Shimadzu UV-3100. ^1H and ^{13}C NMR spectra were recorded on Bruker WF-250 and Bruker AMX-400 in CDCl_3 and CD_3CN solution. The solvent signal was used as internal reference at δH : 7.26 ppm and δC : 77.0 ppm (CDCl_3) and δH : 1.96 ppm and δC : 1.2 and 118.1 (CD_3CN). Cyclic voltammograms were obtained with an Autolab system (PGSTAT 100) in acetonitrile and dichloromethane (0.1 M tetrabutylammonium hexafluorophosphate, TBAH) at 25°C. A three-electrode cell was used comprising a 1 mm Pt-disk working electrode, a Pt wire auxiliary electrode, and an aqueous saturated calomel (SCE) reference electrode. EPR experiments were performed with a Bruker X-band ESP 300 E fitted out with a Bruker B-NM20 gaussmeter. The external magnetic field was calibrated with a microwave bridge EIP548 wavemeter.

2.3. Syntheses

2.3.1. 4-Iodophenylcyanamide (IpcydH)

IpcydH was prepared via the general procedure given for phenylcyanamide derivatives [9]. Benzoyl chloride (12.6 g, 0.09 mol) in acetone (100 cm^3) was added dropwise to a magnetically stirred, refluxing solution of ammonium thiocyanate (6.8 g, 0.09 mol) in acetone

(100 cm^3). After complete addition of the benzoyl chloride, the reaction mixture was allowed to reflux 10 min. 4-Iodoaniline (18.9 g, 0.09 mol) in acetone (50 cm^3) was added dropwise to the refluxing reaction mixture and the reflux was kept for 45 min. The solution turned brown. The product was then poured into cold water (800 cm^3) to ensure complete precipitation of the yellow thiourea derivative. Vigorous stirring was necessary to solubilize the NH_4Cl by-product. The product was filtered, washed with water and dried under vacuum (31.6 g, 96%).

The thiourea derivative (7.3 g, 19 mmol) was dissolved in 2M sodium hydroxide (200 cm^3) by boiling for 10 min. The solution was cooled to 65°C, and a solution of lead(II) acetate trihydrate (7.2 g, 19.1 mmol) in water (60 cm^3) was slowly added. The reaction was allowed to continue for 7 min, the black lead sulfide precipitate was filtered and the filtrate was cooled in an ice bath. Glacial acetic acid (25 ml) was added to neutralize the filtrate and precipitate the neutral ligand. The white product was filtered, washed copiously with cold water and air-dried. $[\text{I}(\text{C}_6\text{H}_4)\text{NHCN}]$ (4.0 g, 87%), Dec. pt 95°C (Found: C, 34.6; H, 2.1; N, 11.1% $\text{C}_7\text{H}_5\text{IN}_2$ requires C, 34.5; H, 2.1; N, 11.5%); IR ν/cm^{-1} 2239s ($\text{C}\equiv\text{N}$); EI mass spectrum m/z 244.0 requires 244.0; $\delta_{\text{H}}(\text{CDCl}_3)$ 7.64 (d, 2Hm, $J=8.99$ Hz), 6.75 (d, 2Ho, $J=8.99$ Hz), 6.15 (s, 1H, N–H), $\delta_{\text{C}}(\text{CDCl}_3)$ 139.0 Cm, 137.4 C_1 , 117.8 Co, 110.9 $\text{C}\equiv\text{N}$, 86.8 Cp.

2.3.2. $[\text{Ru}(\text{tpy})(\text{bpy})(\text{Ipcyd})]\text{PF}_6$

The synthesis was adapted from a literature procedure [10]. To deaerated acetone (100 cm^3) were added 506 mg of $[\text{Ru}(\text{tpy})(\text{bpy})\text{Cl}]\text{PF}_6$ (0.75 mmol) and a slight molar excess of AgPF_6 (1.0 mmol), the resulting solution was then refluxed with stirring for 4 h under argon. A tenfold excess of ligand IpcydH (7.5 mmol) was added, and the solution was stirred under argon with reflux for 4 h, then at room temperature overnight. The precipitated AgCl was removed by filtration on Celite, solid NH_4PF_6 was added to the filtrate, and the solution concentrated to 50 cm^3 . Diethyl ether (300 cm^3) was added. After stirring, the orange precipitate was filtered, washed with diethyl ether and dried under vacuum.

The complex was purified by column chromatography (acidic alumina, $\text{CH}_3\text{CN} + \text{C}_6\text{H}_5\text{CH}_3$; 40/60), the yellow ligand being separated from the dark red complex. Recrystallisation was achieved by diffusing toluene into an acetonitrile solution of the complex. Black needles (518.9 mg, 78%) were obtained. (Found: C, 44.0; H, 2.1; N, 11.5% $\text{C}_{32}\text{H}_{23}\text{IN}_7\text{F}_6\text{PRu}$ requires C, 43.7; H, 2.6; N, 11.1%); IR ν/cm^{-1} 2175s and 2150w (NCN); ES mass spectrum (CH_3CN) m/z : 734.0 $[\text{M} - \text{PF}_6]^+$ requires 734.0; $\delta_{\text{H}}(\text{CD}_3\text{CN})$: 9.74 (1H, d, 5.78 Hz), 8.61 (d, 1H, 8.17 Hz), 8.51 (d, 2H, 7.97 Hz), 8.40

(d, 2H, 7.97 Hz), 8.31 (m, 2H), 8.15 (t, 1H, 7.77 Hz), 7.95 (m, 3H), 7.71 (m, 3H), 7.33 (m, 3H), 6.99 (t, 1H, 5.58 Hz), phenyl ring: 7.10 (2H, d, 8.77 Hz) and 5.88 (2H, d, 8.77 Hz); $\delta_c(\text{CD}_3\text{CN})$ bpy ring: 158.5 Cf, 156.2 Ce, 152.6 Ca, 152.2 Cj, 137.2 Cc, 136.4 Ch, 127.7 Cb, 126.5 Ci, 124.1 Cd, 123.6 Cg, tpy ring: 158.7 C₂, 158.1 C_{2'}, 152.8 C₆, 134.9 C_{4'}, 138.0 C₄, 127.9 C₅, 124.2 C₃, 123.2 C_{3'}, ligand, 137.6 Cm, 122.0 Co, 152.2 C₁, 77.7 Cp.

2.4. Crystal structure determination of $[\text{Ru}(\text{tpy})(\text{bpy})(\text{Ipcyd})]\text{PF}_6$

Dark prismatic crystals of the complex were grown by slow diffusion of toluene in an acetonitrile solution of the complex. A summary of the crystal data is given in Table 1. The diffraction intensities were collected [11] on a Nonius KappaCCD diffractometer at 293 K with molybdenum radiation (0.71073 Å). The structure was solved by direct methods [12] and successive difference Fourier maps. The PF_6^- anion was found severely disordered around the phosphorus atom. It was modelled over two sites with occupation factors of 0.5. The fluorine atoms were then refined isotropically with soft restrains [13]. H atoms were recalculated after each refinement cycle. Refinement was done by full matrix least squares. Calculations were performed with the Crystals Package [14]. The full experimental details, atomic parameters and the complete listing of bond lengths and angles are available as supplementary data. The refinement of this structure is slightly high with $R_f = 0.065$ and this may result from disorder of the

PF_6^- counterion as shown by high residual electron density around the phosphorus atom.

2.5. EPR measurements

$[\text{Ru}(\text{bpy})(\text{tpy})\text{Cl}]\text{PF}_6$ was oxidized totally by electrolysis in dichloromethane and frozen in liquid nitrogen before being analyzed at 100 K. A signal of Ru(III) was observed. Because of its instability, $[\text{Ru}(\text{bpy})(\text{tpy})(\text{Ipcyd})]^{2+}$ was partially generated electrochemically in situ in the EPR tube at 273 K, then the temperature was allowed to decrease until 100K during the electrolysis. A signal with a g near the 2.0023 free electron value was observed, then the product was warmed until 273 K and frozen again, then no more signal was observed. The simulations were obtained with SIMFONIA software [15].

2.6. Extended Hückel calculation

Extended Hückel calculation was made on $[\text{Ru}(\text{bpy})(\text{tpy})(\text{Ipcyd})]^+$ using the crystallographic coordinates. Standard parameters were used, except for ruthenium atom where we took -12.5 eV for the Ru(4d) orbital as suggested by Launay et al. [16]. Molecular orbitals have been visualized with the cacao software [17]. ZINDO/1 calculation was performed by using hyperchem software [18] with default parameters. The shape of the resulting HOMO and LUMO are in perfect agreement with EH results.

3. Results and discussion

3.1. Synthesis and characterization

The procedure is an adaptation of the synthesis of chalcogenoether complexes [10]. The Ru(II) complex is synthesized by a reaction involving Ag(I) abstraction of chloride from $[\text{Ru}(\text{bpy})(\text{tpy})\text{Cl}]^+$ in acetone. Introduction of the IpcydH ligand in tenfold excess leads to the desired complex. Unlike Crutchley's phenylcyanamides [19], iodophenylcyanamide is stable at 60°C so the Ru(II) complex can be formed at acetone refluxing temperature; high purity and good yields are obtained. Deprotonation of the ligand is proved by the observation of the ν_{NCN} band around 2150 cm^{-1} in the IR spectrum of the complex, compared to the neutral ligand vibration ν_{CN} at 2239 cm^{-1} [9]. According to literature, this ν_{NCN} band is shifted to lower energies (ca. 2080–2100 cm^{-1}) for Ru(III) pentaammine compounds [4].

^1H NMR of the complex (Fig. 1) allows an easy distinction of the chloride precursor by the doublets of the phenyl protons from the ligand Ipcyd at 7.10 and 5.88 ppm. Those signals are coupled with a constant

Table 1
Crystallographic data and refinement parameters

Formula	$\text{C}_{32}\text{H}_{23}\text{F}_6\text{IN}_7\text{PRu}$
Crystal system	monoclinic
F_w (g mol^{-1})	878.52
Space group	$P2_1/c$
a (Å)	11.4153(1)
b (Å)	13.2964(1)
c (Å)	23.52561(3)
β (°)	100.9175(6)
V (Å ³)	3506.22(6)
Z	4
$\mu(\text{Mo K}\alpha)$ (cm^{-1})	1.44
ρ_{calc} (g cm^{-3})	1.66
$2\theta_{\text{max}}$ (°)	60.24
Total no. of reflections	250081
R_{int}	0.018
No. of unique reflections with $I > 4\sigma(I)$	7107
Absorption correction	spherical
$T_{\text{min/max}}$	0.53/0.57
R_1^a	0.065
R_w^b	0.075
GOF	1.06

^a $R_1 = \sum ||F_o| - |F_c|| / \sum |F_o|$.

^b $R_w = (\sum w|F_o| - |F_c|)^2 / \sum w|F_o|^2)^{1/2}$.

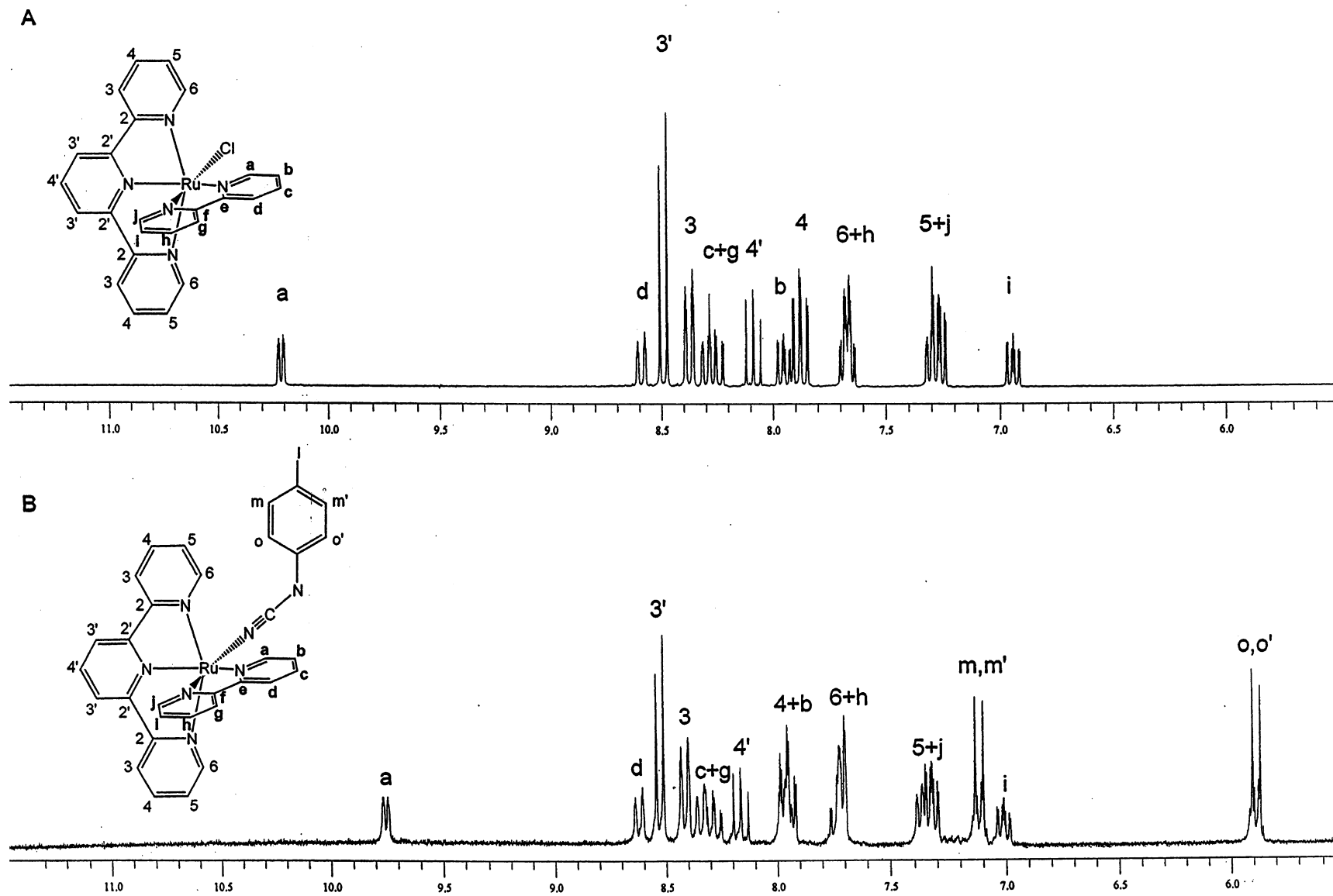


Fig. 1. ^1H NMR of $[\text{Ru}(\text{bpy})(\text{tpy})\text{Cl}]\text{PF}_6$ (A) and $[\text{Ru}(\text{bpy})(\text{tpy})(\text{Ipcyd})]\text{PF}_6$ (B) in CD_3CN .

Table 2
Selected bond lengths (Å) and bond angles (°)^a

Bond lengths			
Ru(1)–N(16)	2.068(3)	Ru(1)–N(69)	2.078(3)
Ru(1)–N(26)	1.970(3)	N(67)–C(66)	1.395(6)
Ru(1)–N(36)	2.073(3)	N(67)–C(68)	1.294(6)
Ru(1)–N(46)	2.053(3)	N(69)–C(68)	1.133(5)
Ru(1)–N(56)	2.076(3)		
Bond angles			
N(16)–Ru(1)–N(26)	79.87(14)	N(46)–Ru(1)–N(56)	78.55(14)
N(16)–Ru(1)–N(36)	159.50(13)	N(16)–Ru(1)–N(69)	88.22(14)
N(26)–Ru(1)–N(36)	79.65(13)	N(26)–Ru(1)–N(69)	90.98(13)
N(16)–Ru(1)–N(46)	93.09(14)	N(36)–Ru(1)–N(69)	91.25(13)
N(26)–Ru(1)–N(46)	95.68(13)	N(46)–Ru(1)–N(69)	73.33(14)
N(36)–Ru(1)–N(46)	89.81(13)	N(56)–Ru(1)–N(69)	94.79(14)
N(16)–Ru(1)–N(56)	102.98(13)	Ru(1)–N(69)–C(68)	174.5(3)
N(26)–Ru(1)–N(56)	173.63(13)	N(67)–C(68)–N(69)	173.0(5)
N(36)–Ru(1)–N(56)	97.49(13)	C(66)–N(67)–C(68)	120.4(4)

^a Angle between the C(61)–C(66) mean plane and the tpy mean plane: 103.3(1)°. Angle between the C(61)–C(66) mean plane and the bpy mean plane: 27.9(1)°. Torsion angle C(68)–N(67)–C(66)–C(65): 7.0(3)°.

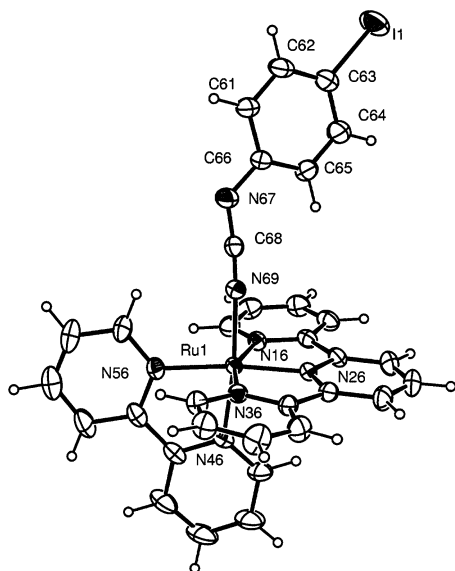


Fig. 2. ortep drawing of the cation [Ru(bpy)(tpy)(Ipcyd)]⁺ along with the atom numbering scheme (probability level of 30%).

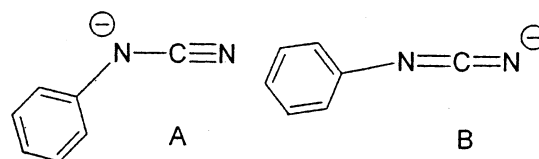
$J_{\text{HH}} = 8.77$ Hz. The H_a bipyridine proton which points toward the ligand is characteristic. It undergoes the influence of the substituent because of its privileged position; the crystal structure shows a short intramolecular contact of 2.636(3) Å between N69 of the cyanamide ligand and H55 (the one attached to C55) of the bipyridine moiety (see crystal structure section). The upfield shift from 10.2 to 9.74 ppm upon substitution of the chloride atom by the Ipcyd molecule is due to the larger diamagnetic anisotropy of iodophenylcyanamide vs. chloride [20]. The assignments of the remaining

bipyridine and terpyridine protons come from correlation spectroscopy (COSY). The ¹³C NMR signal assignments were based on the heteronuclear 2D ¹H–¹³C correlation spectroscopy (HMQC and HMBC).

Electrospray mass spectrum is consistent with the formula. It shows the molecular peak positively charged by the loss of the hexafluorophosphate ion at m/z : 734 and the fragment [Ru(bpy)(tpy)]⁺ at m/z : 490.

3.2. X-ray structure

Crystal structure data for [Ru(bpy)(tpy)(Ipcyd)]PF₆ and selected bond lengths and angles are respectively given in Tables 1 and 2. Fig. 2 shows the ortep [21] drawing of the [Ru(bpy)(tpy)(Ipcyd)]⁺ cation and the numbering scheme used in Table 2. This structure is similar to the one obtained by Rasmussen et al. for [Ru(tpy)(bpy)(CH₃CN)]²⁺ [22]. Small angle C(66)–N(67)–C(68) (120.4(4)°), long distance N(67)–C(68) (1.294(6) Å), short distance C(68)–N(69) (1.133(5) Å) and the large angle C(68)–N(69)–Ru(1) (174.5(3)°) are consistent with the resonance structure A coordinated to the metal ion via the nitrile lone pair, rather than with the B form [23].



By referring to the Cambridge Structural Database [24], one can observe that the bond distance between N(69) and C(68) is very typical of a CN triple bond in CN–Ru(II) (median value 1.13 Å). The angle between the bipyridine mean plane and the iodophenylcyanamide mean plane is about 30°.

There is an apparent contradiction between X-ray and Infrared data: Infrared data show two distinct absorption bands in KBr disks or nujol mull: a strong one at 2175 cm⁻¹ and a weaker one at 2150 cm⁻¹. The presence of two bands is usually interpreted as the presence of two conformers where cyanamide ligands are inequivalent [4,23]. Note however that this was proposed for Ru(III) complexes. Yet for this study, the X-ray structure strictly demonstrates the presence of only one conformation. In fact, it probably means that the X-ray analysis was made on only one kind of crystals.

3.3. UV–Vis absorption

The [Ru(II)(bpy)(tpy)(Ipcyd)]⁺ spectrum in dichloromethane (Fig. 3) shows, in the visible region; two broad bands (439 and 495 nm). The attribution of the charge transfer transition of [Ru(II)(bpy)(tpy)L]ⁿ⁺ salts has

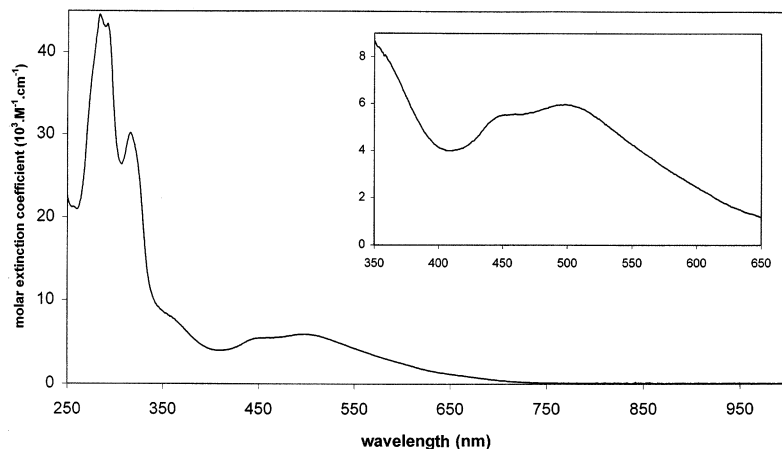


Fig. 3. UV–Vis spectrum of $[\text{Ru}(\text{bpy})(\text{tpy})(\text{Ipcyd})]\text{PF}_6$. Insert: enlargement of the specified area.

Table 3
UV–Vis absorption bands and redox potential

	Absorption bands, λ (nm) ($\epsilon \times 10^{-3}$, $\text{dm}^3 \text{mol}^{-1} \text{cm}^{-1}$)		Electrochemical data, E V/SCE (ΔE , mV)	
	$\pi^* \leftarrow \pi$	Charge-transfer transition	$E_{\text{RuIII/II}}$	
IpcydH in CH_3CN	203 (35), 244 (32), 285 (6.3)			
$[\text{Ru}(\text{II})(\text{bpy})(\text{tpy})(\text{Ipcyd})]^+$ in CH_2Cl_2	242 (26), 283 (44), 316 (30), 358sh (7.1)	MLCT, 498 (6.0), 453 (5.4)	0.698 ^a	-1.38 (70)
$[\text{Ru}(\text{II})(\text{bpy})(\text{tpy})\text{Cl}]^+$ in CH_2Cl_2	240 (41), 282 (38), 294 (43), 318 (38), 360sh (8.6)	MLCT, 505 (12.0)	0.871 (73)	-1.42 (73)
$[\text{Ru}(\text{III})(\text{bpy})(\text{tpy})\text{Cl}]^{2+}$ in CH_3CN	319 (8.2)	LMCT, 402 (2.9)		

^a Anodic potential of the half-wave attributed to an EC mechanism.

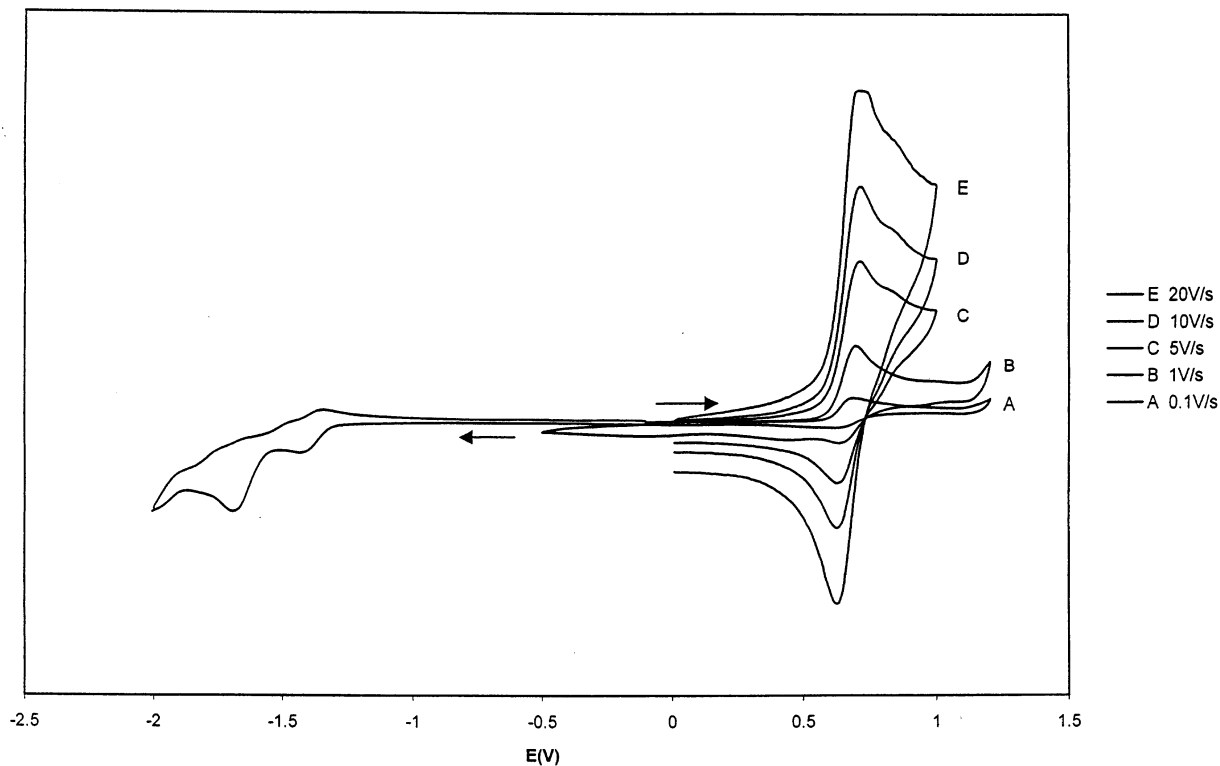


Fig. 4. Cyclic voltammograms of $[\text{Ru}(\text{bpy})(\text{tpy})(\text{Ipcyd})]\text{PF}_6$ in CH_3CN for different scan rates.

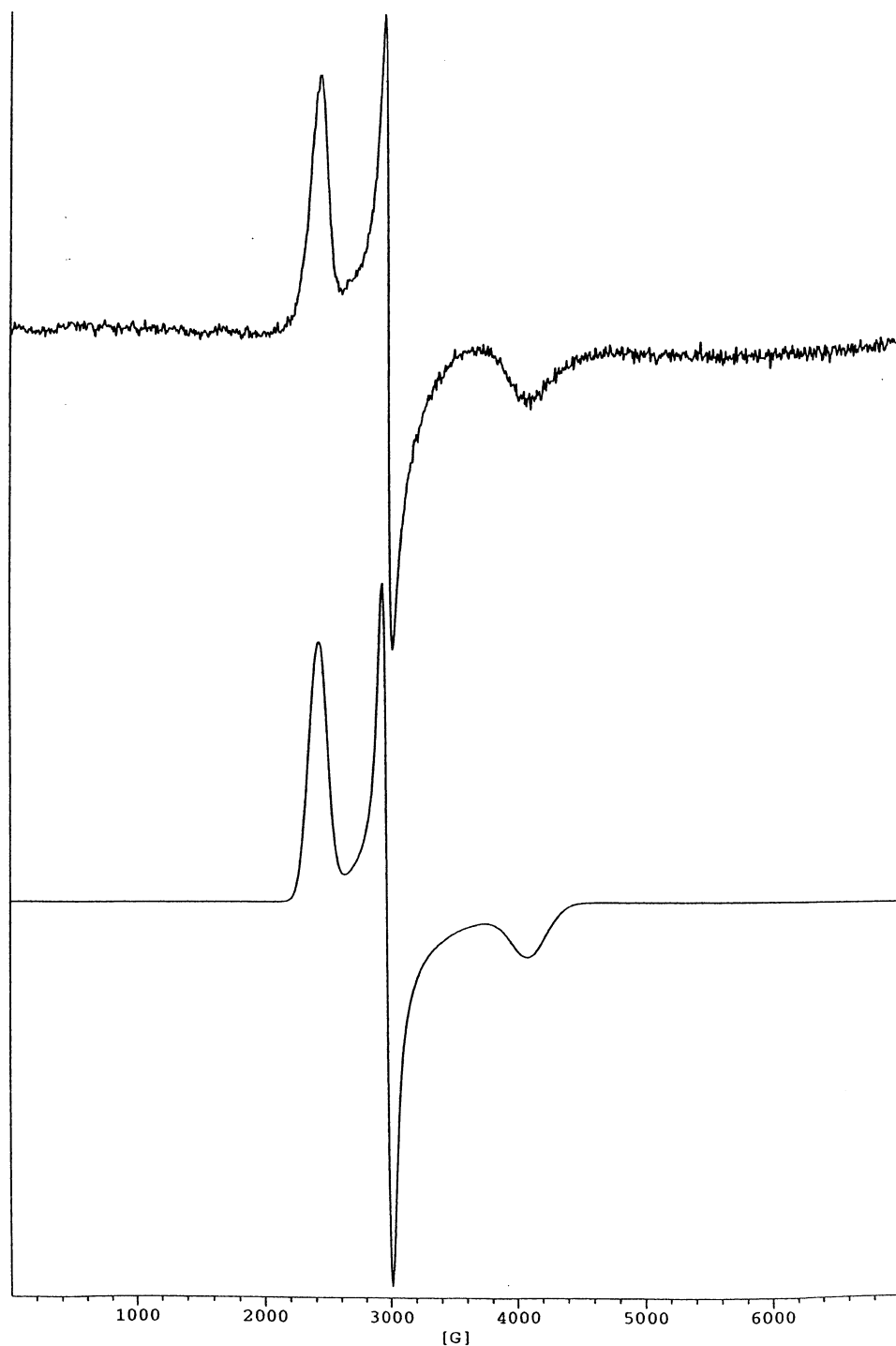


Fig. 5. Experimental (top) EPR spectrum of $[\text{Ru}(\text{bpy})(\text{tpy})\text{Cl}]^{2+}$ in frozen CH_2Cl_2 (100 K) and simulated (bottom).

been largely documented [22,25]. Thus, in the present case, the band at 495 nm can be assigned to $d\pi(\text{Ru}(\text{II})) \rightarrow \pi^*(\text{tpy})$ MLCT transition, indeed tpy moiety presents a more extended π system than bpy one, then gives more stable π^* orbitals and thus lower excited energy state. The second band at 439 nm can be assigned to $d\pi(\text{Ru}(\text{II})) \rightarrow$

$\pi^*(\text{bpy})$ transition. The absence of solvatochromism on these bands corroborates these attributions.

Upon oxidation, the large MLCT band of the chloro complex disappears and a smaller band at 402 nm assigned to a ligand $\pi \rightarrow d\pi(\text{Ru}(\text{III}))$ (LMCT) charge transfer transition grows.

3.4. Electrochemistry

Cyclic voltammetry (CV) data for the complexes are given in Table 3. The $E_{1/2}$ potentials were determined from the average of the anodic and cathodic peak potentials except for $[\text{Ru}(\text{bpy})(\text{tpy})(\text{Ipcyd})]^{+/2+}$ which shows an irreversible wave where only the anodic peak

is observed. Successive ligand-based reductions are observed in the negative region. These reductions correspond to the formation of radical anions as electrons are added to the π^* orbitals of the polypyridyl ligands. The first wave, well-defined, has been assigned to terpy reduction [26] in agreement with the calculation described below. The other waves, less well-resolved espe-

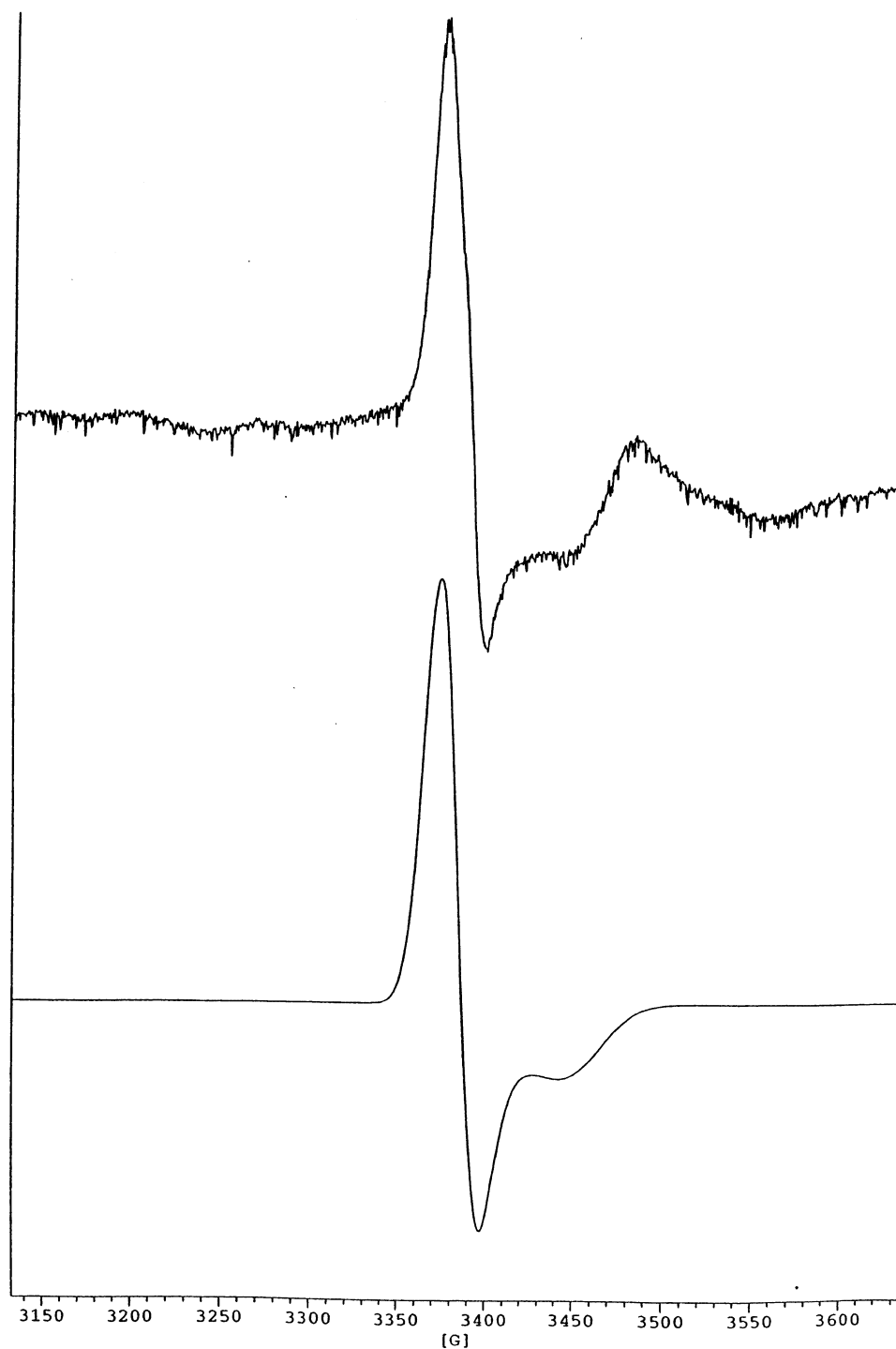


Fig. 6. Experimental (top) EPR spectrum of $[\text{Ru}(\text{bpy})(\text{tpy})(\text{Ipcyd})]^{2+}$ in frozen CH_2Cl_2 (100 K) and simulated (bottom).

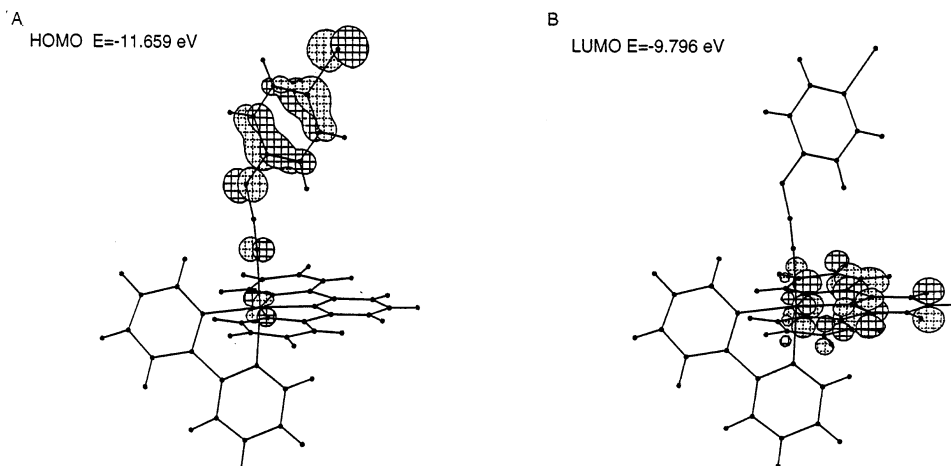


Fig. 7. Results from Extended Hückel calculation for $[\text{Ru}(\text{bpy})(\text{tpy})(\text{Ipcyd})]^+$: (A) HOMO; (B) LUMO.

cially in dichloromethane, are assumed to correspond to bpy and tpy reductions, respectively.

The anodic peak around 0.7 V/ECS could at first sight be assigned to the oxidation of the ruthenium atom of the iodide complex. This wave is shifted to less positive potentials (ca. 150 mV) compared to the case of $[\text{Ru}(\text{bpy})(\text{tpy})\text{Cl}]^{+/2+}$. This would agree with the more donor character of the iodophenylcyanamide ligand compared to the chloro.

Fig. 4 shows the behavior of the wave at different scan rates. The reversibility of the wave at 0.7 V/ECS increases with increasing scan rate, this takes evidence for an electrochemical–chemical reaction. From those CV, an approximate half-life time in the order of seconds has been measured for the primary electrochemically generated species [27].

3.5. EPR measurements

The EPR spectrum of electrogenerated $[\text{Ru}(\text{bpy})(\text{tpy})\text{Cl}]^{2+}$ is very typical of a low-spin d^5 Ru(III) ion [28] with $g_x = 2.79$; $g_y = 2.23$ and $g_z = 1.61$ (Fig. 5). In contrast, the EPR spectrum of $[\text{Ru}(\text{bpy})(\text{tpy})(\text{Ipcyd})]^{2+}$ shows an axial signal at $g_{\perp} = 2.00$ and $g_{\parallel} = 1.96$ (Fig. 6), which can be taken as an evidence for the presence of an organic radical. It would be generated as the primary species and would subsequently transform to the secondary species, which is EPR silent (see Section 2.5).

This assumption about an organic radical formation is substantiated further by extended Hückel and ZINDO/1 calculations showing the HOMO (Fig. 7(a)) largely dominated by the phenylcyanamide contribution. This tends to prove that the ligand should be oxidized first rather than the metal. It also can be noted that the LUMO (Fig. 7(b)) is dominated by the ter-

pyridine fragment. This corroborates the terpyridine reduction assignment in CV experiment.

4. Conclusion

In conclusion, full characterization including X-ray structure determination has been made on the title complex. CV, EPR, Hückel and ZINDO calculations converge to the fact that oxidation of the title compound leads to an unprecedented Ru complex with the cyanamido organic radical. This last species seems to be unstable according to the CV and EPR results, and the desired paramagnetic Ru(III) complex is not obtained. Nevertheless, the chemical ability of the title compound to give Sonogashira coupling reactions has been demonstrated and yields a new class of compounds which will be described elsewhere. For the future, attempts will be made to add donor substituents on terminal polypyridine entities in order to lower the oxidation potential of the Ru(II/III) couple in order to avoid the formation of unwanted unstable organic radical. Once obtained the desired functionalized mononuclear species, the next step will be to make a long binuclear molecule and then study magnetic and electronic coupling.

5. Supplementary material

Crystallographic data for the structural analysis have been deposited with the Cambridge Crystallographic Data Centre, CCDC no. 157364. Copies of this information may be obtained from The Director, CCDC, 12 Union Road, Cambridge, CB2 1EZ, UK (fax: +44-1233-336033; e-mail: deposit@ccdc.cam.ac.uk or www: <http://www.ccdc.cam.ac.uk>).

Acknowledgements

We thank Dominique de Montauzon (Laboratoire de Chimie de Coordination, Toulouse) for electrochemical advice and facilities, Alain Mari (Laboratoire de Chimie de Coordination, Toulouse) for EPR measurements and Christophe Coudret (CEMES) for helpful suggestions regarding synthetic strategies.

References

- [1] (a) N.S. Hush, *Prog. Inorg. Chem.* 8 (1967) 391. (b) S. Woitellier, J.-P. Launay, C.W. Spangler, *Inorg. Chem.* 28 (1989) 758.
- [2] (a) T.R. Felthouse, D.N. Hendrickson, *Inorg. Chem.* 17 (1978) 2636. (b) R.J. Crutchley, *Adv. Inorg. Chem.* 41 (1994) 273.
- [3] P.K.A. Shonfield, A. Be-hrendt, J.C. Jeffery, J.P. Maher, J.A. McCleverty, E. Psillakis, M.D. Ward, C. Western, *J. Chem. Soc., Dalton Trans.* (1999) 4341.
- [4] M.A.S. Aquino, F.L. Lee, E.J. Gabe, C. Bensimon, J.E. Greedan, R.J. Crutchley, *J. Am. Chem. Soc.* 114 (1992) 5130.
- [5] A.R. Revzani, C.E.B. Evans, R.J. Crutchley, *Inorg. Chem.* 34 (1995) 4600.
- [6] K. Sonogashira, Y. Tohda, N. Hagihara, *Tetrahedron Lett.* 50 (1975) 4467.
- [7] B.P. Sullivan, J.M. Calvert, T.J. Meyer, *Inorg. Chem.* 19 (1980) 1404.
- [8] J.M. Calvert, H.S. Russell, B.P. Sullivan, J.S. Facci, T.J. Meyer, R.W. Murray, *Inorg. Chem.* 22 (1983) 2151.
- [9] M.L. Naklicki, R.J. Crutchley, *Inorg. Chem.* 28 (1989) 1955.
- [10] M.J. Root, E. Deutsch, *Inorg. Chem.* 24 (1985) 1464.
- [11] Z. Otwinowski, W. Minor, in: C.W. Carter, R.M. Sweet (Eds.), *Methods Enzymol.*, vol. 276, Academic Press, New York, 1997, p. 307.
- [12] A. Altomare, G. Cascarano, G. Giacovazzo, A. Guagliardi, M.C. Burla, G. Polidori, M. Camalli, *J. Appl. Cryst.* 27 (1994) 435.
- [13] J.R. Carruthers, D.J. Watkin, *Acta Crystallogr., Sect. A* 35 (1979) 698.
- [14] D.J. Watkin, C.K. Prout, J.R. Carruthers, P.W. Betteridge, *Crystals*, Chemical Crystallography Laboratory, Oxford, UK, Issue 10, 1997.
- [15] WINEPR SIMFONIA ver. 1.25, Bruker Analytische Messtechnik GmbH, 1996.
- [16] C. Patoux, J.-P. Launay, M. Beley, S. Chodorowski-Kimmes, J.-P. Collin, S. James, J.-P. Sauvage, *J. Am. Chem. Soc.* 120 (1998) 3717.
- [17] C. Mealli, D.M. Proserpio, *J. Chem. Educ.* 67 (1990) 399.
- [18] Hyperchem™ release 6.01 for Windows, Chemcad, 2000 Hypercube, Inc.
- [19] M.L. Naklicki, R.J. Crutchley, *Inorg. Chem.* 28 (1989) 4226.
- [20] A. Gerli, J. Reedijk, M.T. Lakin, A.L. Spek, *Inorg. Chem.* 34 (1995) 1836.
- [21] L.J. Farrugia, *J. Appl. Cryst.* I (1997) 565.
- [22] S.C. Rasmussen, S.E. Ronco, D.A. Mlsna, M.A. Bil-ladeau, W.T. Pennington, J.W. Kolis, J.D. Petersen, *Inorg. Chem.* 34 (1995) 821.
- [23] R.J. Crutchley, R. Hynes, E.J. Gabe, *Inorg. Chem.* 29 (1990) 4921.
- [24] F.H. Allen, O. Kennard, *Chem. Des. Automation News* 8 (1993) 31.
- [25] (a) K.J. Takeuchi, M.S. Thompson, D.W. Pipes, T.J. Meyer, *Inorg. Chem.* 23 (1984) 1845. (b) N.C. Fletcher, F.R. Keene, *J. Chem. Soc., Dalton Trans.* (1998) 2293; P.A. Anderson, G.F. Strouse, J.A. Treadway, F.R. Keene, T.J. Meyer, *Inorg. Chem.* 33 (1994) 3863. (c) S. Ruile, O. Khole, P. Pécny, M. Gratzel, *Inorg. Chim. Acta* 261 (1997) 129. (d) C.R. Hecker, P.E. Fanwick, D.R. Mc Millin, *Inorg. Chem.* 30 (1991) 659. (e) A. Ben Altabel, S.B. Ribotta de Gallo, M.E. Folquer, N.E. Katz, *Inorg. Chim. Acta* 188 (1991) 67. (f) P.A. Anderson, G.B. Deacon, K.H. Haarmann, F.R. Keene, T.J. Meyer, D.A. Reitsma, B.W. Skelton, G.F. Strouse, N.C. Thomas, T.A. Treadway, A.H. White, *Inorg. Chem.* 34 (1995) 6145.
- [26] R.M. Berger, D.R. McMillin, *Inorg. Chem.* 27 (1988) 4245.
- [27] R.S. Nicholson, I. Shain, *Anal. Chem.* 36 (1964) 706.
- [28] (a) J.S. Griffith, *The Theory of Transition-Metal Ions*, Ch. 12, Cambridge University Press, London, 1961, pp. 346–374. (b) J.B. Raynor, B.G. Jeliaskowa, *J. Chem. Soc., Dalton Trans.* (1982) 1185.